Received: 22 December 2021 | Revised: 9 June 2022 | Accepted: 22 July 2022

DOI: 10.1111/gbi.12522

gebiology WILEY

ORIGINAL ARTICLE

Physiological and metabolic responses of chemolithoautotrophic NO_3^- reducers to high hydrostatic pressure

Ileana Pérez-Rodríguez[1,2] | Stefan M. Sievert[3] | Marilyn L. Fogel[2,4,†] | Dionysis I. Foustoukos[2]

[1]Department of Earth and Environmental Science, University of Pennsylvania, Philadelphia, Pennsylvania, USA

[2]Earth and Planets Laboratory, Carnegie Institution of Washington, Washington, District of Columbia, USA

[3]Biology Department, Woods Hole Oceanographic Institution, Woods Hole, Massachusetts, USA

[4]Department of Earth and Planetary Sciences, University of California, Riverside, California, USA

Correspondence
Ileana Pérez-Rodríguez, Department of Earth and Environmental Science, University of Pennsylvania, 264 A Hayden Hall, 240 South 33rd Street, Philadelphia, PA 19104-6316, USA.
Email: ileperez@sas.upenn.edu

Funding information
Carnegie Institution of Washington; Center for Dark Energy Biosphere Investigations; NASA Exobiology Award, Grant/Award Number: 80NSSC21K0485; NASA Astrobiology Institute; National Science Foundation, Grant/Award Number: OCE 1038114, OCE 1136608, BIO-1951673 and OCE 1038131; University of Pennsylvania Elliman Faculty Fellowship; WHOI Investment in Science Fund

Abstract

We investigated the impact of pressure on thermophilic, chemolithoautotrophic NO_3^- reducing bacteria of the phyla *Campylobacterota* and *Aquificota* isolated from deep-sea hydrothermal vents. Batch incubations at 5 and 20 MPa resulted in decreased NO_3^- consumption, lower cell concentrations, and overall slower growth in *Caminibacter mediatlanticus* (*Campylobacterota*) and *Thermovibrio ammonificans* (*Aquificota*), relative to batch incubations near standard pressure (0.2 MPa) conditions. Nitrogen isotope fractionation effects from chemolithoautotrophic NO_3^- reduction by both microorganisms were, on the contrary, maintained under all pressure conditions. Comparable chemolithoautotrophic NO_3^- reducing activities between previously reported natural hydrothermal vent fluid microbial communities dominated by *Campylobacterota* at 25 MPa and *Campylobacterota* laboratory isolates at 0.2 MPa, suggest robust similarities in cell-specific NO_3^- reduction rates and doubling times between microbial populations and communities growing maximally under similar temperature conditions. Physiological and metabolic comparisons of our results with other studies of pressure effects on anaerobic chemolithoautotrophic processes (i.e., microbial S^0-oxidation coupled to Fe(III) reduction and hydrogenotrophic methanogenesis) suggest that anaerobic chemolithoautotrophs relying on oxidation–reduction (redox) reactions that yield higher Gibbs energies experience larger shifts in cell-specific respiration rates and doubling times at increased pressures. Overall, our results advance understanding of the role of pressure, its relationship with temperature and redox conditions, and their effects on seafloor chemolithoautotrophic NO_3^- reduction and other anaerobic chemolithoautotrophic processes.

KEYWORDS
anaerobic chemolithoautotrophy, cell-specific respiration rates, deep-sea hydrothermal vents, doubling times, high hydrostatic pressure, N isotopes, NO_3^- reduction

†Deceased.

1 | INTRODUCTION

High hydrostatic pressure (HHP) is a notable physical parameter associated with anaerobic chemolithoautotrophic processes at deep-sea hydrothermal vent ecosystems. Although pressure is a key parameter, most of our knowledge on the metabolic and physiological behavior of anaerobic chemolithoautotrophic microorganisms from deep-sea vents has been generated through laboratory experiments with cultures and microcosms near standard pressure (~0.2 MPa) conditions (e.g., Bourbonnais et al., 2012; Fortunato & Huber, 2016; Hoek et al., 2006; Jannasch, 1983, 1995; Pérez-Rodríguez et al., 2017; Sievert & Vetriani, 2012; Stewart et al., 2019; Topçuoğlu et al., 2016; Ver Eecke et al., 2012). Integrating HHP into physiological studies of anaerobic chemolithoautotrophs has been complicated by the technical difficulties associated with HHP microbial cultivation, and by the low numbers of laboratory HHP studies focused on anaerobic chemolithoautotrophy (Houghton et al., 2007; Takai et al., 2008, 2009). Recent HHP experiments and in situ studies using natural deep-sea vent microbial communities (Bourbonnais et al., 2012; Breusing et al., 2020; Fortunato et al., 2021; McNichol et al., 2016, 2018) provide a new avenue for linking the metabolic and physiological behaviors of anaerobic chemolithoautotrophs documented in the laboratory with those operating in situ.

Here, we investigate the effect of pressure on microbial respiration rates, cell yields, doubling times, and N isotope fractionation effects during chemolithoautotrophic NO_3^- reduction by cultured bacterial species of the phyla *Campylobacterota* and *Aquificota*—known to dominate anaerobic chemolithoautotrophic processes at deep-sea hydrothermal vent environments (Bourbonnais et al., 2012; Campbell et al., 2006; Fortunato & Huber, 2016; Nakagawa et al., 2005; Nakagawa & Takai, 2008; Pérez-Rodríguez et al., 2013; Schrenk et al., 2010; Sievert & Vetriani, 2012). Placed in context with HHP incubations of (i) natural hydrothermal fluid communities performing chemolithoautotrophic NO_3^- reduction (McNichol et al., 2016, 2018) and of (ii) other anaerobic chemolithoautotrophic processes (Takai et al., 2008; Zhang et al., 2018), our results help to illuminate the combined effect of catabolic redox reactions, temperature, and pressure on the growth and metabolic activities of anaerobic chemolithoautotrophs.

2 | MATERIALS AND METHODS

2.1 | Bacterial strains and culture conditions

Caminibacter mediatlanticus strain TB-2^T (DSM 16658; Voordeckers et al., 2005) of the phylum *Campylobacterota* and *Thermovibrio ammonificans* strain HB-1^T (DSM 15698; Vetriani et al., 2004) of the phylum *Aquificota* were selected as model organisms to study the effects of HHP on chemolithoautotrophic NO_3^- reduction. *C. mediatlanticus* (thermophile, T_{opt} = 55°C) and *T. ammonificans* (extreme thermophile, T_{opt} = 75°C) are strict anaerobes capable of H_2 oxidation coupled to dissimilatory NO_3^- reduction to NH_4^+ (DNRA). *C. mediatlanticus* and *T. ammonificans* were grown in SME medium (Stetter et al., 1983) modified for optimal growth at pH 5.5, and salinities of 3% w/v and 2% w/v NaCl, respectively (Vetriani et al., 2004; Voordeckers et al., 2005). Anoxic conditions for *C. mediatlanticus* and *T. ammonificans* were established using a gas phase of H_2/CO_2 (80%: 20% v/v, 0.2 MPa) with $H_{2(aq)}$ (~1 mM) as primary electron donor (PED), CO_2 (~15 mM of $CO_{2(aq)} + HCO_3^-$) as carbon source (C source), and NO_3^- (~14 mM) as terminal electron acceptor (TEA).

2.2 | Bacterial cultivation and monitoring at high hydrostatic pressure

Culturing at HHP was performed using a Dickson-type flexible gold-titanium (Au/Ti) reaction cell with a maximum working volume of ~50 ml (Foustoukos et al., 2015; Seyfried et al., 1979, 1987; Zhang et al., 2018). Experimental HHP conditions were established through the addition of H_2O into the pressure reactor within the Au/Ti reaction cell (Figure S1). A band heater externally applied to the pressure vessel, subsequently enclosed in an insulated furnace, was used to set and maintain experimental temperatures. A thermocouple placed in direct contact with the pressure medium (H_2O) was used to monitor and control the temperature through the band heater during time-series experiments.

C. mediatlanticus and *T. ammonificans* were each incubated within the Au/Ti reaction cell at their respective optimal growth temperature (T_{opt}) conditions and at varying pressures of 0.2, 5, and 20 MPa. The highest applied experimental pressure (equivalent to 2000 m water depth) represented in situ seafloor conditions similar to those from which *C. mediatlanticus* (2305 m) and *T. ammonificans* (2500 m) were isolated (Vetriani et al., 2004; Voordeckers et al., 2005). Incubations were established by filling the flexible Au cell compartment with 40 ml of anoxic growth medium and 0.8 ml of a culture pre-grown for 16 h (corresponding to mid-exponential growth phase cells), all prepared under anoxic conditions (gas headspace H_2/CO_2; 80%: 20% v/v, 0.2 MPa). Anoxic conditions were maintained by continuously flushing the Au cell compartment with H_2/CO_2 as the anoxic, resazurin-containing (1 mg/L) medium and inoculum were added. Once sealed (0.2 MPa headspace pressure with H_2/CO_2), starting experimental conditions (time at zero hours) were measured before establishing desired HHP conditions as the reaction cell heated to the desired temperature. Continuous monitoring was required during this time in order to maintain desired HHP conditions by removing excess H_2O upon media heating. Desired temperatures and HHP conditions were reached after ~1.5 h under low heating rates to ensure a smooth transition into experimental conditions. Pre-heating the culture established in the sealed Au cell compartment in a regular incubator before assembly into the Au/Ti reaction cell (not done in this study) may help shorten the pressure setup step.

To monitor the physiological and metabolic responses to pressure over time during batch incubations, sampling was conducted through a valve directly linked to the Au/Ti reaction cell.

Immediately before each sample was taken, the culture was mixed by turning the Au/Ti reaction cell upside down several times. Pressure conditions during sampling were maintained by simultaneously adding H_2O to the pressure vessel during sample retrieval. To prevent damage from deformability of the Au cell compartment, subsampling was constrained to 20–30 ml of the total liquid volume. All experimental time series were performed at least twice, and all the resulting data were used for our analyses, unless stated otherwise (in Tables S1–S3). Cell concentrations were monitored through direct cell counts of culture samples (0.5 ml) fixed with 25 µl of 25% v/v glutaraldehyde and stained with 0.1% (w/v) acridine orange. Stained cells filtered onto a 0.2 µm pore size black polycarbonate filter were visualized under an Olympus BX61 Fluorescence Microscope with an oil immersion objective lens (UPlanF1 100/1.3). All HHP cultures were transferred after 52 h of incubation into Balch tubes containing 10 ml of fresh medium and incubated at 0.2 MPa to test for cell viability (qualitatively via turbidity observations) after exposure to HHP.

2.3 | NO_3^- and NH_4^+ concentration measurements

Samples (1 ml each) were retrieved at different times during incubations for measurements of cell-free NO_3^- and NH_4^+. All samples were passed through 0.2 µm pore-size regenerated cellulose (4 mm) syringe filters before being stored at −20°C. Filtered samples for NH_4^+ analyses were treated with 10 µl of 2 M HCl before freezing. Nitrate concentrations were determined using ion chromatography (Metrohm, "MIC-3 Advanced IC", Metrosep A supp 7-250 column) with an estimated uncertainty (2σ) of <2%. Ammonium concentrations were determined with the indophenol blue method (Solorzano, 1969) via spectrophotometry (Labsystems Multiskan MCC/340 Microplate Reader) at 640 nm. Spectrophotometric measurements were performed as duplicates for each sample and reported as average values.

2.4 | NO_3^- and NH_4^+ extractions for stable N isotope analyses

To measure the isotopic composition of N in cell-free NO_3^- and NH_4^+, each compound was individually pre-concentrated in 1 cm diameter glass fiber disks grade GF/D filters for mass spectrometry analyses (1–10 µmol typically required; Holmes et al., 1998). Extractions were carried out separately for NO_3^- and NH_4^+ using the NO_3^- extraction method (Sigman et al., 1997) and the NH_4^+ diffusion protocol (Holmes et al., 1998) as described by Pérez-Rodríguez et al. (2017).

GF/D disks containing the extracted dissolved inorganic compounds were placed in 5 × 9 mm pressed silver caps, to capture any chloride impurities (Gandhi et al., 2004; Johnson et al., 2018) during combustion in a Carlo-Erba NC2500 elemental analyzer. The N isotopic composition of combusted samples were analyzed relative to a N_2 reference gas by a ThermoFisher Delta V Plus isotope ratio mass spectrometer. Experimental standards (and positive controls for NO_3^- and NH_4^+ extractions) were prepared by adding NO_3^- or NH_4^+ from a stock solution with known isotopic compositions to de-ionized water in order to achieve NO_3^- and NH_4^+ concentrations similar to that expected in the starting media. Initial NO_3^- and NH_4^+ concentrations in the cultures were ~14 and ~0.16 mM, respectively. Acetanilide (C_8H_9NO) was also analyzed at regular intervals to monitor the accuracy of the measured isotopic ratios and elemental compositions. All data are reported in δ notation, in units of permil (‰) relative to N_2 in air, as $\delta^{15}N = [(R_{sample}/R_{air}) - 1] * 1000‰$, where $R = {}^{15}N/{}^{14}N$. Experimental $\delta^{15}N$ standard controls averaged 1.0 ± 0.66‰ ($n = 15$) for NH_4^+ and 2.1 ± 0.29‰ ($n = 15$) for NO_3^- across all isotope ratio mass spectrometry runs. Mean precision (1σ) of $\delta^{15}N$ values from acetanilide internal standards are shown in Tables A1 and A2 of the electronic annex.

First order kinetics was assumed for the closed system conditions associated with microbial NO_3^- reduction experiments, where a finite amount of NO_3^- was irreversibly metabolized. A Rayleigh fractionation model was applied to describe the kinetic fractionation of N between NO_3^- and evolved NH_4^+ (Guy et al., 1993; Kendall & Caldwell, 1998; Maggi & Riley, 2010). Stable N isotope fractionations associated with NO_3^- reduction were then determined using the following equation (Kinnaman et al., 2007; Mariotti et al., 1981):

$$\varepsilon = \frac{10^3 \times \ln \frac{10^{-3}\delta^{NO_3^-} + 1}{10^{-3}\delta^{NO_3^-}{}_{initial} + 1}}{\ln(f)} \quad (1)$$

where $\delta^{NO_3^-}$ is the $\delta^{15}N$ of NO_3^- and f is the fraction of unreacted NO_3^- remaining at time (t) during the reaction (Mariotti et al., 1981). The N isotope effect, ε, is defined as $[({}^{14}k/{}^{15}k) - 1] \times 1000‰$, where ${}^{14}k$ and ${}^{15}k$ refer to the reduction rates for ${}^{14}NO_3^-$ and ${}^{15}NO_3^-$, respectively. This was calculated from the corresponding slope of the linear function of the numerator and the denominator in Equation (1). This linear expression passing through the origin assumes a constant kinetic fractionation effect at each experimental condition (Mariotti et al., 1981). Uncertainties on these estimations are expressed as 2σ standard deviation of the fitted slope, which takes into account the analytical uncertainties of the measured $\delta^{15}N$ values.

2.5 | Data analysis for metabolic and physiological parameters

Doubling times from specific growth rates (h^{-1}) of exponentially growing cells in batch cultures were calculated as previously performed by Pérez-Rodríguez et al. (2017):

$$k = \frac{\ln(C_x) - \ln(C_0)}{t_x - t_0} \quad (2)$$

where t_0 and t_x are the start of exponential growth and the time (h) of sampling, respectively. C_0 and C_x are cell concentrations (number of

cells/ml) at time t_0 and t_x, respectively. Doubling times are expressed as ln(2)/k. Exponential growth started within hours after inoculation at 0.2 MPa, so time 0 h was set as t_0 for all assays.

Cell yields (number of cells/mol of reduced NO_3^-) were calculated as the ratio of the increase in the number of cells and of the NH_4^+ produced as previously performed by Sim et al. (2011) and Pérez-Rodríguez et al. (2017):

$$Y = \frac{C_x - C_0}{[NH_4^+]_x - [NH_4^+]_0} \quad (3)$$

Cell-specific NO_3^- reduction rates (csNRR; $\mu mol \times 10^{-9}$/cell/h or fmol/cell/h) were calculated from the obtained specific growth rates in Equation (2) and cell yields in Equation (3) (Pérez-Rodríguez et al., 2017; Sim et al., 2011):

$$csNRR = k / Y = \frac{\ln(C_x) - \ln(C_0)}{t_x - t_0} \bullet \frac{[NH_4^+]_x - [NH_4^+]_0}{C_x - C_0} \quad (4)$$

NO_3^- reduction kinetic rate constants were defined by the slope of the linear function between $\ln[NO_3^-] \times 10^{-3}$ versus time (h), assuming first order reaction kinetics (McQuarrie & Simon, 1997), as described by Pérez-Rodríguez et al. (2017).

Doubling times, cell yields, and csNRRs associated with DNRA-based and overall NO_3^- reduction activities were also calculated from published data on HHP (25 MPa) batch incubations of natural hydrothermal vent fluid microbial communities from the East Pacific Rise (EPR), metabolizing over 24 h at 24°C or 50°C (Table S3; McNichol et al., 2016). Data associated with csNRRs and cell yields from DNRA activities were calculated using Equations (3) and (4). Data associated with csNRRs and cell yields from overall NO_3^- reduction activities were calculated using the absolute values of the consumption of NO_3^- with time in Equations (3) and (4), instead of the NH_4^+ produced over time.

Doubling times (h), cell yields (number of cells/µmol of TEA), and cell-specific respiration rates (csRRs; $\mu mol \times 10^{-9}$/cell/h or fmol/cell/h) were also calculated using data obtained from HHP batch incubation experiments with (i) laboratory-generated, mixed mesophilic and acidophilic communities incubated at 30°C for ~22 days in a similar Dickson-type flexible Au/Ti cell with S^0 as an PED, Fe(III) as a TEA and CO_2 as the C source (Zhang et al., 2018), and (ii) hydrogenotrophic methanogenic populations (H_2 as PED and CO_2 as TEA/C source) of *Methanopyrus kandleri* growing optimally at 105°C for up to 10 h (Takai et al., 2008) using a piezophilic cultivation syringe system (Marteinsson et al., 1997; Table S3). Data from Zhang et al. (2018) were obtained from Figure 5 of their publication using GetData Graph Digitizer software (http://www.getdata-graph-digitizer.com/). Data from Takai et al. (2008) and McNichol et al. (2016) were taken directly from the provided supplementary information.

3 | RESULTS

3.1 | Growth at 0.2, 5, and 20 MPa

Batch culture incubations showed that HHP conditions (5 and 20 MPa) affected the growth of *C. mediatlanticus* and *T. ammonificans*. Only a small increase in cell numbers was observed for *C. mediatlanticus* and *T. ammonificans* at elevated pressures with no obvious changes in batch growth phases (Figure S2 top panel), compared to the substantial increase in cell numbers and distinct batch growth phases usually observed at 0.2 MPa (this study; Pérez-Rodríguez et al., 2017; Vetriani et al., 2004; Voordeckers et al., 2005). Decreased cell concentrations at HHP were also associated with increases in overall doubling times. The shortest doubling times for replicated *C. mediatlanticus* experiments averaged 4.1 ± 0.5 h at 0.2 MPa, 13.6 ± 2.3 h at 5 MPa, and 40.7 ± 19.6 h at 20 MPa, while for *T. ammonificans* the shortest doubling times averaged 3.3 ± 1.0 h at 0.2 MPa, 18.4 ± 16.8 h at 5 MPa, and 40.2 ± 24.4 h at 20 MPa. Growth was difficult to assess at elevated pressures due to the pressure manipulations required for the adopted HHP sampling procedure (Taylor & Jannasch, 1976). However, HHP samples (0.2 ml) used as inocula (taken at 52 h of incubation) in 10 ml of liquid media under standard laboratory conditions showed culture viability in all instances. Clear evidence of growth from turbidity observations and documented increase in cell numbers by *C. mediatlanticus* and *T. ammonificans* were also consistently obtained once the HHP batch system was disassembled and opened at the end of the experiments (see asterisks in plots b and c of Figure S2). Therefore, cell concentrations acquired from HHP samples during the experiments were likely underestimates, possibly due to cell lysis. A different procedure consisting of a set of three micrometering valves, applied to a different HHP cultivation setup (Foustoukos & Pérez-Rodríguez, 2015), could—in principle—improve the retrieval of subsamples from the Au/Ti reaction cell (by avoiding the exposure of collected biomass to shear forces).

3.2 | Chemolithoautotrophic NO_3^- reduction at 0.2, 5, and 20 MPa

Overall NO_3^- consumption by *C. mediatlanticus* averaged 5.02 ± 1.87 mM after 52 h for replicates at 0.2 MPa, 2.24 ± 0.51 mM after 76 h for replicates at 5 MPa, and 1.96 ± 0.63 mM after 96 h for replicates at 20 MPa. In *T. ammonificans* replicates, overall NO_3^- consumption averaged 12.90 ± 3.31, 1.23 ± 0.79, and 2.02 ± 0.61 mM after 52 h under 0.2 MPa, after 72 h under 5 MPa, and after 96 h under 20 MPa, respectively. The comparatively smaller fraction of NO_3^- consumed by *C. mediatlanticus* (~50% less NO_3^- than at 0.2 MPa) and *T. ammonificans* (~75% less NO_3^- than at 0.2 MPa) at elevated

pressure (Figure S2 bottom panel) is also associated with comparatively lower cell concentrations in cultures grown at 5 and 20 MPa. Decreased NO_3^- consumption (Figure S2e,f) and NH_4^+ production (Figure S3) at elevated pressure also translated into one order of magnitude lower NO_3^- reduction rates compared to those observed at 0.2 MPa (Figure S4). Specifically, DNRA rate constants describing the growth of *C. mediatlanticus* went from $0.03 \pm 0.01\,h^{-1}$ for replicates at 0.2 MPa to $0.003 \pm 0.001\,h^{-1}$ for replicates at 5 MPa and $0.002 \pm 0.000\,h^{-1}$ for replicates at 20 MPa. DNRA rate constants for *T. ammonificans* cultures decreased from $0.052 \pm 0.004\,h^{-1}$ for replicates at 0.2 MPa to $0.002 \pm 0.001\,h^{-1}$ for replicates at 5 MPa and $0.003 \pm 0.000\,h^{-1}$ for replicates at 20 MPa.

3.3 | Cell-specific NO_3^- reduction rates and cell yields at 0.2, 5, and 20 MPa

At 0.2 MPa, *T. ammonificans* showed higher csNRRs and lower cell yields compared to *C. mediatlanticus*, as previously described in Pérez-Rodríguez et al. (2017). At elevated pressures, csNRRs decreased in both *C. mediatlanticus* and *T. ammonificans* (Figure 1a,b). These differences are more pronounced and likely significant in *T. ammonificans* cultures between 72 and 120 h under HHP conditions (Figure 1b). Calculations using cell concentrations obtained from samples taken once the HHP system was disassembled (asterisks in Figure 1) also suggest potential significant csNRR differences in *C. mediatlanticus* cultures between 72 and 120 h under HHP conditions. The lowest csNRR values at 0.2 MPa were associated with late exponential growth phases, while csNRR values became progressively lower in association with HHP incubations despite not showing distinct batch growth phases. It appears that HHP cultures mostly remained in either lag phase or early-exponential phase throughout the duration of the experiments with overall lower maximal cell concentrations than those attained in cultures at 0.2 MPa by 24 h. However, csNRR differences in *C. mediatlanticus* and *T. ammonificans* at different pressures did not appear to translate into differences in cell yields despite the variability observed in panels c and d of Figure 1. Most cell yield values obtained from HHP samples taken once the Au/Ti reaction cell was disassembled (asterisks in Figure 1c,d) appear comparable to cell yield values from cultures incubated at 0.2 MPa. The possibility of underestimated cell concentrations from sampling under HHP conditions (based on higher cell concentrations obtained once the Au/Ti reaction cell was disassembled) means that microbial csNRRs may actually have been lower than reported in our study while cell yields may have been higher than reported (more like asterisks in Figure 1).

3.4 | N isotope effects of DNRA at different hydrostatic pressures

A normal kinetic isotope effect, calculated from changes in NO_3^- concentrations and its N isotope composition with time, was observed in *C. mediatlanticus* and *T. ammonificans* at 0.2 MPa, as previously reported (Pérez-Rodríguez et al., 2017). In *C. mediatlanticus*, enrichment factors (ε) averaged from 6.1 ± 0.6‰ for replicates at 0.2 MPa to 5.3 ± 3.8‰ for replicates at 5 MPa and 7.8‰ (single growth experiment) at 20 MPa (Figure 2a–c). *T. ammonificans* displayed ε values from 7.2 ± 0.3‰ for replicates at 0.2 MPa to 6.7 ± 5.9‰ for replicates at 5 MPa and 5.9‰ (single growth experiment) at 20 MPa

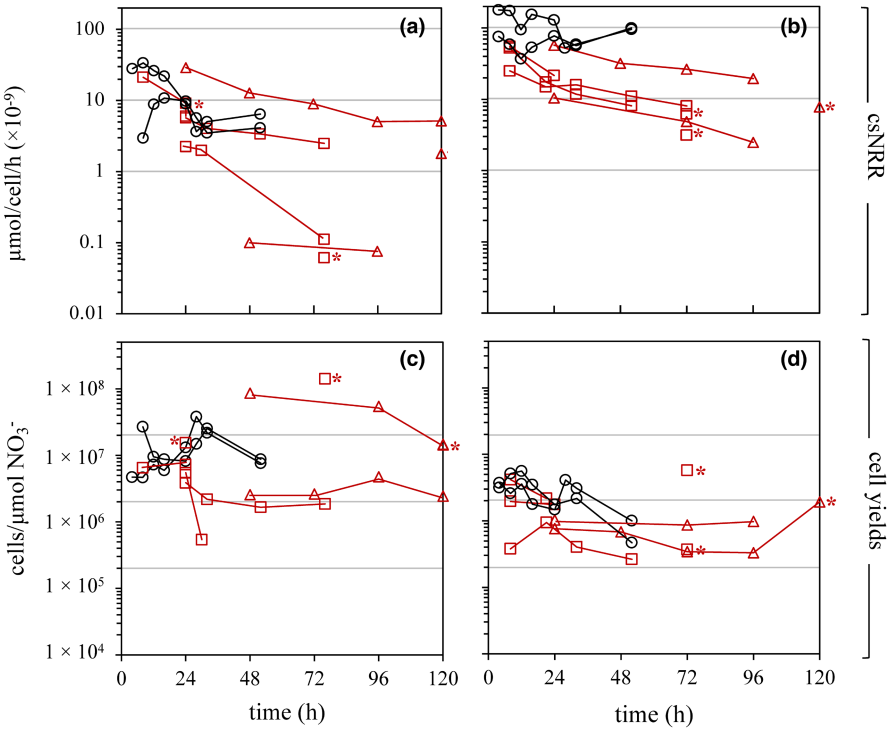

FIGURE 1 Cell-specific NO_3^- reduction rates (a,b) and cell yields (c,d) for *Caminibacter mediatlanticus* (a,c) and *Thermovibrio ammonificans* (b,d) incubated near standard pressure (0.2 MPa, black circles) and under HHP conditions (5 MPa, red squares and 20 MPa, red triangles). Asterisks represent data calculated with cell concentration (cells/ml) values from samples obtained once the HHP batch system was disassembled and opened at the end of the experiments

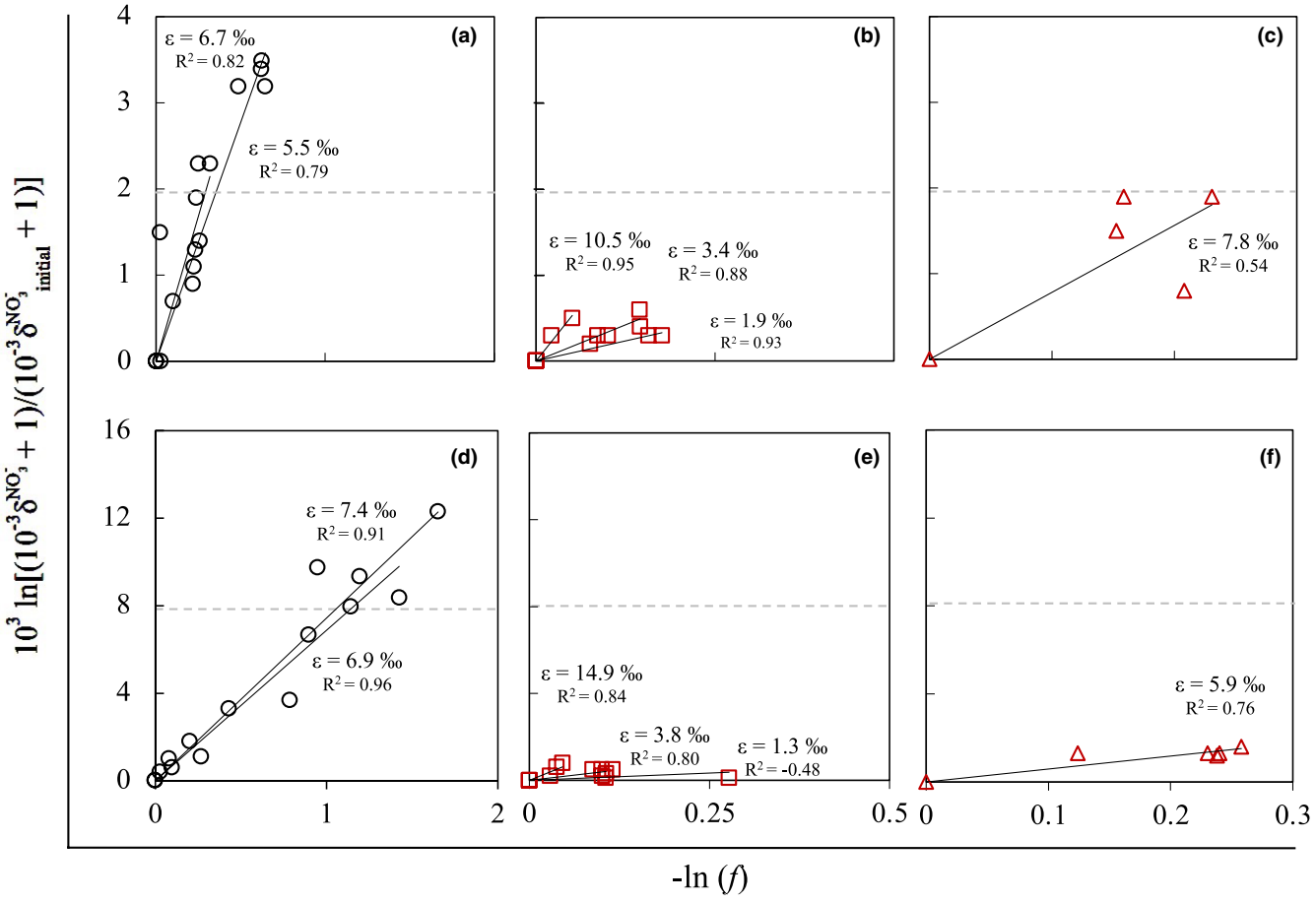

FIGURE 2 Enrichment factors (ε) for stable N isotopes in cell-free NO_3^- during chemolithoautotrophic NO_3^- reduction activities by *Caminibacter mediatlanticus* (a–c) and *Thermovibrio ammonificans* (d–f) incubated at 0.2 MPa (a,d), 5 MPa (b,e) and 20 MPa (c,f)

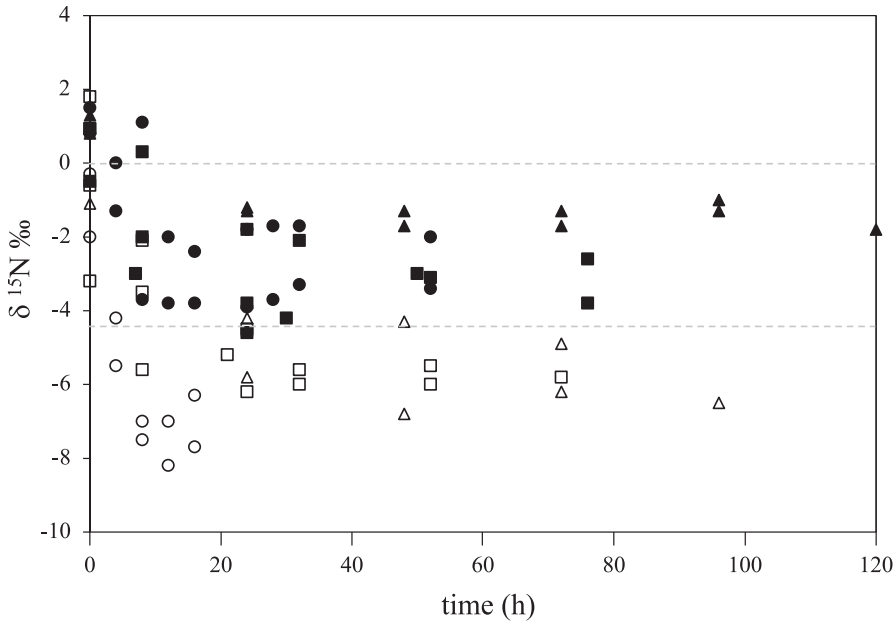

FIGURE 3 Stable N isotopes of produced NH_4^+ during DNRA activities by *Caminibacter mediatlanticus* (solid symbols) and *Thermovibrio ammonificans* (open symbols) at 0.2 MPa (circles), 5 MPa (squares) and 20 MPa (triangles)

(Figure 2d–f). These values exclusively represent NO_3^- pools in the media, given that no NO_2^- was detected via ion chromatography in our experiments. Most ε values are statistically not significantly supported ($r^2 < 0.95$), likely due to (i) small experimental datasets, (ii) low resolution in determining N isotope changes from the small absolute changes of NO_3^- concentrations in HHP cultures, and (iii) the

lack of continuous stirring of the cultures during incubations. The NH_4^+ produced during DNRA by each organism was, on the contrary, consistently depleted in ^{15}N under all pressure conditions (Figure 3), in line with N kinetic isotope effects reported previously at 0.2 MPa (Pérez-Rodríguez et al., 2017).

3.5 | Chemolithoautotrophic NO_3^- reduction in pure cultures versus mixed natural communities from deep-sea hydrothermal vents

Previously published data (Table S3) from HHP batch incubations (25 MPa) of natural microbial communities in hydrothermal vent fluids from the EPR (McNichol et al., 2016) were used to compare pure cultures (present study) to mixed natural communities. We assumed that (i) the experimental addition of NO_3^- to hydrothermal fluids limited by TEA supply in situ (McNichol et al., 2016) and (ii) the documented dominance of *Campylobacterota* (~86% to 100% of the *Bacteria*, which made up 94% to 100% of the total community) in the HHP hydrothermal fluid incubations (McNichol et al., 2016, 2018), allowed for comparative analysis with pure cultures of NO_3^- reducing *Campylobacterota*.

Calculated csNRRs and cell yields from NO_3^- reduction activities in pure cultures and from HHP hydrothermal fluid incubations over 24 h at 24°C or 50°C (McNichol et al., 2016; Table S3) are shown in Figure 4. Values specific to DNRA activities (based on the microbial production of NH_4^+) in hydrothermal fluid incubations at 50°C (green data points in Figure 4a,b)—dominated by members of the order *Nautiliales*, like *C. mediatlanticus*, known to perform DNRA (McNichol et al., 2018)—fully overlap with values from DNRA activities by *C. mediatlanticus* growing at 55°C. Calculated DNRA-based csNRRs and cell yields from hydrothermal fluid incubations at 50°C aligned more closely with csNRRs and cell yields observed in the pure culture at 0.2 MPa (black open circles in Figure 4a,b). Overall csNRRs and cell yields (based on the microbial consumption of NO_3^-) from HHP hydrothermal fluid incubations at 24°C (Figure 4c,d)—represented by denitrifying members of the genera *Sulfurimonas* and *Sulfurovum* (McNichol et al., 2018)—generally overlap with previously reported values from denitrifying activities by *Sulfurimonas paralvinellae* (× symbols) and *Sulfurovum lithotrophicum* (star symbols) growing at 30°C and 0.2 MPa (Inagaki et al., 2004;

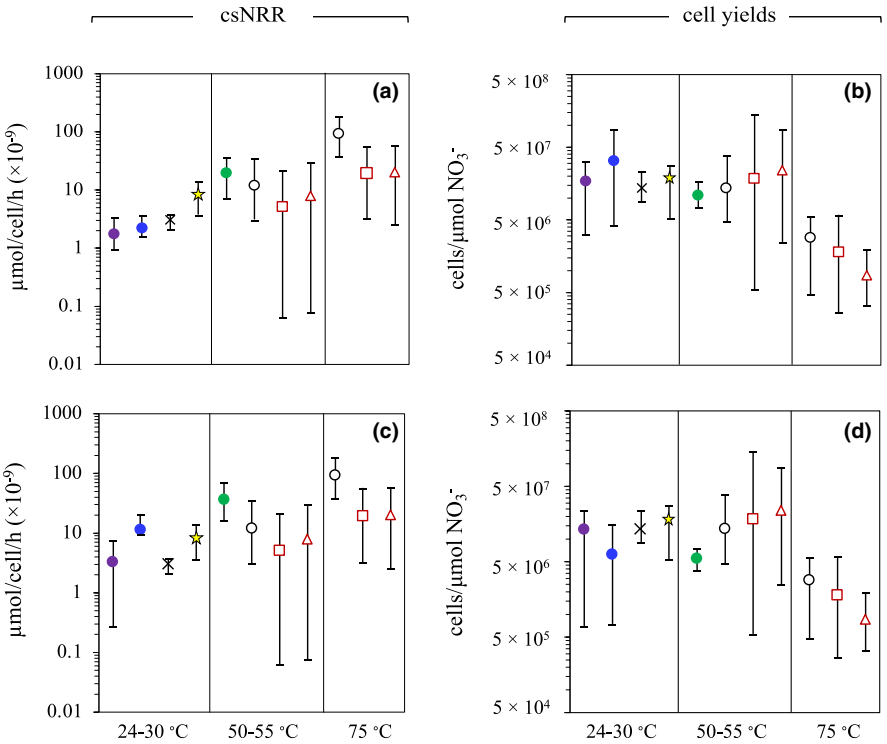

FIGURE 4 Averaged cell-specific NO_3^- reduction rates (a,c) and cell yields (b,d) from DNRA-based (a,b) and overall NO_3^- reduction activities (c,d) associated with HHP hydrothermal fluid incubations enriched in NO_3^- at 24°C (solid purple circles), H_2 and NO_3^- at 24°C (solid blue circles) and H_2 and NO_3^- at 50°C (solid green circles). DNRA-based NO_3^- reduction activities refer to the production of NH_4^+, whereas overall NO_3^- reduction activities refer to the overall microbial consumption of NO_3^-. Comparison with laboratory pure cultures include this study on *Caminibacter mediatlanticus* (at 55°C) and *Thermovibrio ammonificans* (at 75°C) growing near standard pressure (0.2 MPa, black open circles) and at HHP conditions (5 MPa, red open squares and 20 MPa, red open triangles). Also displayed are csNRRs and cell yields of *Sulfurovum lithotrophicum* (star symbols) and *Sulfurimonas paralvinellae* (× symbol) growing via denitrification at 30°C and 0.2 MPa. Bars represent maximal and minimal values associated with averaged csNRRs and cell yields (not standard deviations)

Pérez-Rodríguez et al., 2017; Takai et al., 2006). Higher overall csNRRs (Figure 4c,d) versus DNRA-based csNRRs (Figure 4a,b) in HHP hydrothermal fluid incubations at 24°C are consistent with previous conclusions that denitrification dominated NO_3^- reduction activities in HHP incubations at 24°C (McNichol et al., 2016, 2018). Higher overlap between DNRA-based csNRRs (Figure 4a,c) in HHP hydrothermal fluid incubations at 50°C with DNRA-based csNRRs in *C. mediatlanticus* also reflect previous conclusions that DNRA dominated NO_3^- reduction activities in HHP hydrothermal fluid incubations at 50°C (McNichol et al., 2016, 2018).

The shortest doubling times observed in HHP incubations with natural communities at 24°C ranged from 18.2 ± 4.5 h when supplemented with excess NO_3^- to 4.0 ± 0.4 h when supplemented with an excess of both NO_3^- and H_2 (McNichol et al., 2016; Table S3). These values overlap with the documented doubling times of 17.5 h for *S. paralvinellae* and 3.7 ± 1.7 h for *S. lithotrophicum*, both growing at 30°C and 0.2 MPa (Pérez-Rodríguez et al., 2017; Takai et al., 2006). The shortest doubling times observed in HHP hydrothermal fluid incubations at 50°C were 3.3 ± 0.6 h (McNichol et al., 2016; Table S3), which is comparable to the doubling times observed in *C. mediatlanticus* growing at 55°C and 0.2 MPa (4.1 ± 0.5 h).

3.6 | The effect of pressure on anaerobic chemolithoautotrophic metabolisms

Additional comparisons with HHP batch incubations of (i) a laboratory-generated acidophilic community performing S^0-oxidation coupled to Fe(III) reduction at 30°C (Zhang et al., 2018) and (ii) *M. kandleri* performing hydrogenotrophic methanogenesis at T_{opt} of 105°C (Takai et al., 2008) show that microorganisms achieve cell yields between 1×10^6 and 1×10^7 cells per μmol of TEA despite pressure changes (Figure 5 bottom panel). However, a pronounced temperature dependence can be observed in csRRs per fmol (or μmol × 10^{-9}) of TEA (Figure 5 top panel), despite differences in pressure conditions or chemolithoautotrophic reactions. These csRR patterns are maintained after correcting for differences in the number of electrons transferred during catabolism (Figure S5). Except for *C. mediatlanticus*, cell yields are also maintained after normalizing chemolithoautotrophic reactions as electron transfers (Figure S5).

The shortest doubling times associated with S^0-oxidizing, Fe(III)-reducing growth were 61.4 h at 0.2 MPa and 166.6 h at 10 MPa. This shift toward slower overall growth rates also coincided with lower cell concentrations (maximum of 4.5×10^7 cells/ml) and lower overall production of Fe(II) during respiration (9.7 mM) at HHP versus cell concentrations (maximum of 1.3×10^8 cells/ml) and Fe(II) produced (32 mM) at 0.2 MPa during the same time interval of ~22 h (Zhang et al., 2018). The shortest doubling times associated with *M. kandleri* remained the same (1.2 h at 2 MPa and 1.1 ± 0.3 h between 10 and 50 MPa) regardless of pressure conditions (Takai et al., 2008).

4 | DISCUSSION

4.1 | Effects of pressure and temperature on chemolithoautotrophic NO_3^- reduction

C. mediatlanticus and *T. ammonificans* appeared to slow csNRRs and doubling times as pressure conditions increased from 0.2 MPa to either 5 MPa or 20 MPa (Figure 1). Decreases in csNRRs and overall doubling times from experimental HHP manipulations could result from pressure-related changes in enzyme-catalyzed reaction rates via structural enzymatic changes (Balny et al., 1997; Meersman et al., 2013; Oger & Jebbar, 2010; Silva & Weber, 1993). Pressure changes are also known to induce alterations in membrane permeability and thus affect transport processes across the cell membrane (Barlett et al., 1995; Meersman et al., 2013; Oger & Jebbar, 2010). Macromolecular changes resulting from pressure changes (from room pressure to experimental HHP conditions) at the start of each experiment could lead to sudden changes in intracellular metabolic fluxes and an overall imbalance between anabolism and catabolism (Abe, 2007). Indeed, microbial pressure responses appear to involve large-scale metabolism modifications with no characteristic signature of "high-pressure"-induced genes (Charlesworth & Burns, 2016; Jebbar et al., 2015; Oliver et al., 2020; Zhang et al., 2015). The decrease in csNRRs and overall doubling times at HHP might reflect a microbial response to intracellular redox imbalances from initial pressure-induced changes during the experimental setup, in the effort to maintain somewhat similar cell yields per unit of NO_3^- metabolized despite pressure changes (Figure 1c,d). Lower csNRRs and overall doubling times resulting from pressure-induced changes in enzymatic rates might also serve as a mechanism to alleviate initial intracellular redox imbalances by slowing down catabolism (and overall doubling times). It is unknown whether longer incubation times at HHP, or repeated transfers of viability cultures at HHP, would allow pure cultures to eventually reach similar csNRRs and doubling times as those observed at 0.2 MPa.

The overlap between csNRRs and doubling times in HHP hydrothermal fluid incubations at 24°C with denitrifying activities by *S. paralvinellae* and *S. lithotrophicum* (both displaying T_{opt} of 30°C) at 0.2 MPa, and at 50°C with DNRA activities by *C. mediatlanticus* (T_{opt} = 55°C) at 0.2 MPa (Figure 4), also demonstrates comparable activities by phylogenetically and functionally similar microbial populations and communities growing maximally. Comparative analysis of seafloor (15 MPa) and shipboard (~0.1 MPa) incubations of hydrothermal fluids from Axial Seamount of the Juan de Fuca Ridge, which were primarily composed of anaerobic chemolithoautotrophic *Campylobacterota* (Fortunato & Huber, 2016), have also shown similar microbial-community behavior despite differences in incubation pressures (Fortunato et al., 2021). Observed csNRR patterns in pure cultures at 0.2 MPa and natural communities at 25 MPa (i.e., csNRRs at 75°C > csNRRs between 50°C and 55°C > csNRRs at 24°C and 30°C) also follow previously described patterns of higher csNRRs associated with the growth of deep-sea vent chemolithoautotrophic NO_3^-

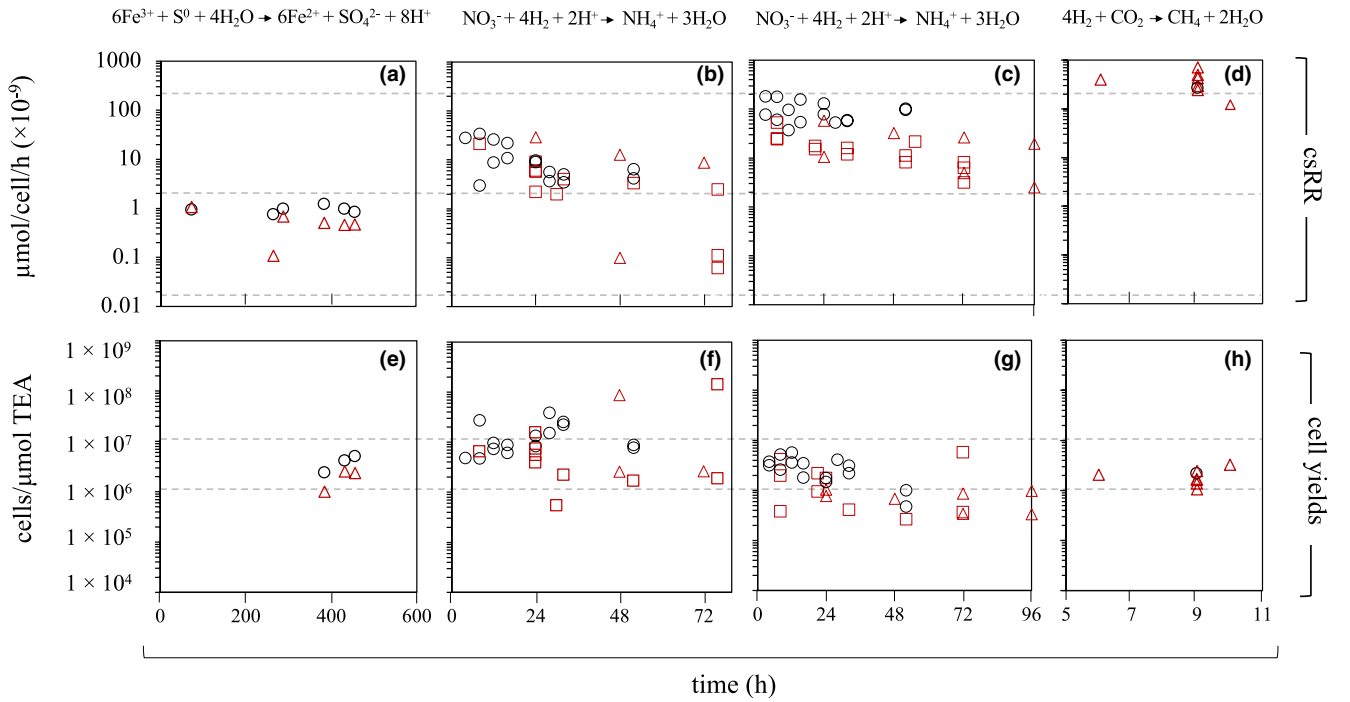

FIGURE 5 Cell-specific respiration rates (csRRs; panels a–d) and cell yields (panels e–h) from S^0-oxidizing, Fe(III)-reducing activities by a mixed mesophilic and acidophilic community at 30°C (a,e), hydrogenotrophic NO_3^- reduction activities by *Caminibacter mediatlanticus* at 55°C (b,f) and *Thermovibrio ammonificans* at 75°C (c,g), as well as hydrogenotrophic methanogenesis by *Methanopyrus kandleri* growing at 105°C (d,h). Data correspond to batch incubations near standard pressure conditions (0.1 to 2 MPa, open black circles) and at HHP conditions (5 MPa, open red squares and 10 to 50 MPa, open red triangles)

reducers at higher temperatures (Pérez-Rodríguez et al., 2017). We hypothesize that deep-sea vent *Campylobacterota* adapted to similar optimal growth temperature conditions display similar baseline csNRRs and maximal doubling times attainable under preferred growth pressure conditions. It is worth noting that HHP hydrothermal fluid incubations by McNichol et al. (2016) never experienced pressure changes in the way laboratory cultures did in this study (from 0.2 MPa to HHP conditions in every assay).

4.2 | Effects of pressure and temperature on other anaerobic chemolithoautotrophic processes

Decreases in csRRs of at least one order of magnitude are observed in association with hydrogenotrophic NO_3^- reduction in response to HHP (Figure 1a,b), while a more moderate shift toward slower csRRs is observed for the culture performing S^0 oxidation coupled with Fe(III) reduction in response to elevated pressure (Figure 5a). Hydrogenotrophic methanogenic activities, on the contrary, generally maintained csRRs independent of pressure conditions (Figure 5d). Overall doubling times associated with hydrogenotrophic methanogenesis occurring at 105°C were also maintained despite pressure changes. S^0-oxidizing/Fe(III)-reducing microorganisms, on the contrary, displayed significantly longer doubling times when growing at HHP conditions. Like *C. mediatlanticus* and *T. ammonificans*, longer doubling times by S^0-oxidizing/Fe(III)-reducing microorganisms at HHP were associated with lower overall cell concentrations developed during anabolism and lower overall product generation (i.e., Fe(II) or NH_4^+) during catabolism. It may be possible that anaerobic chemolithoautotrophs relying on redox reactions with higher Gibbs free energies are able to adapt to HHP changes by altering the coupling between csRRs and cell yields in ways low-energy yielding reactions cannot. Conserved cell-specific CH_4 production rates have already been documented in thermophilic and hyperthermophilic hydrogenotrophic methanogens growing continuously under standard pressures despite differences in dilution rates or temperature conditions (Stewart et al., 2019). The absence of metabolic response by *Methanococcus maripaludis* performing methanogenesis under formate (PED and C source) limitation has also been documented at 30°C and 0.3 MPa (Müller et al., 2021). Additional experimentation will be required to understand the extent to which chemolithoautotrophic NO_3^- reducers can adjust their metabolism to lower energy transfer rates (and thus, longer doubling times) in response to changes in pressure and intracellular redox imbalances or whether this decrease in csNRRs reflects minimal maintenance energy requirements toward in vitro dormancy or death.

4.3 | Stable N isotope effects during chemolithoautotrophic NO_3^- reduction at different pressures

Slower microbial csNRRs and doubling times associated with increased pressure conditions created challenges for us to fully characterize the

kinetic isotope effect from changes in cell-free NO_3^- concentrations and its N isotope composition during DNRA. Specifically, the small absolute changes from the initial cell-free NO_3^- concentrations induced by microbial metabolism—together with our inability to continuously stir the HHP reaction vessel during incubation—likely increased analytical uncertainties because of sample heterogeneity in vitro. However, averaged enrichment factors by *C. mediatlanticus* and *T. ammonificans* at 5 and 20 MPa ranged between 5.3–6.7‰ and 5.9–7.8‰, respectively—in line with overall averaged enrichment factors between 6.1 and 7.2‰ at 0.2 MPa. Both organisms also showed similar N isotope composition patterns for the NH_4^+ produced during DNRA activities regardless of pressure conditions (Figure 3). Because the resulting cell-free NH_4^+ pool was largely established through DNRA, NH_4^+ $\delta^{15}N$ values more reliably documented N kinetic isotope effects from DNRA that were consistent with those reported at 0.2 MPa. We infer that the mechanism by which DNRA occurred within these two phylogenetically distinct microbes (*Campylobacterota* and *Aquificota*) is similar and operates similarly under different pressures despite slower csNRRs and doubling times.

4.4 | Chemolithoautotrophic NO_3^- reduction at deep-sea hydrothermal vents

Chemolithoautotrophic NO_3^- reduction capabilities observed in cultured *Campylobacterota* and *Aquificota* from deep-sea hydrothermal vents (Pérez-Rodríguez et al., 2017; Sievert & Vetriani, 2012) are ecologically relevant given the dominance of these two phyla in deep-sea vent microbial communities at moderate-to-high temperatures (~25 to 80°C) and suboxic/anoxic conditions (Bourbonnais, Juniper, et al., 2012; Bourbonnais, Lehmann, et al., 2012; Campbell et al., 2006; Fortunato & Huber, 2016; McNichol et al., 2016; Nakagawa et al., 2005; Schrenk et al., 2010). Both *Campylobacterota* and *Aquificota* (including *C. mediatlanticus* and *T. ammonificans*) have been shown to encode for Nap periplasmic NO_3^- reductases (Giovannelli et al., 2017; Pérez-Rodríguez et al., 2017; Vetriani et al., 2014) for the first irreversible step in cellular NO_3^- reduction, which also appears to control the observed $^{14}N/^{15}N$ fractionation of NO_3^- respiration (Kritee et al., 2012). A link between *Campylobacterota* and community-level N isotope effects of <3‰ for both NO_3^- and NH_4^+ has already been established in hydrothermal fluids from the Juan de Fuca Ridge (JdFR) ranging from ~6 to 71°C (Bourbonnais, Juniper, et al., 2012). Higher $\delta^{15}N$ NO_3^- values concomitant with decreased NO_3^- concentrations at some JdFR sites were reported to indicate assimilatory or dissimilatory microbial consumption of NO_3^- with relatively low community N isotope effects ($\varepsilon < 3‰$). Low NH_4^+ community N isotope effects of <3‰ were reported to reflect important contribution from gross NH_4^+ regeneration at ≤50°C (Bourbonnais, Lehmann, et al., 2012). The microbial generation of NH_4^+ has also been inferred from the inverse relationship between NH_4^+ concentrations and NO_3^- + NO_2^- concentrations in hydrothermal fluids (at ~20 to 50°C) at the *Lō'ihi* Seamount (Karl et al., 1989; Sedwick et al., 1992; Sylvan et al., 2017). The detection of $\delta^{15}N$ NH_4^+ values (0.0 and 3.3‰) lower than background seawater $\delta^{15}N$ NO_3^- values (~6‰) in *Lō'ihi* hydrothermal fluids between 30 and 40°C (Sylvan et al., 2017) and the increasing proportion of *Campylobacterota* detected in *Lō'ihi* hydrothermal fluids ≥40°C (Emerson & Moyer, 2002; Moyer et al., 1994, 1998), also support the link between *Campylobacterota* and N cycling at deep-sea vents. No N isotope systematics have been documented to date for high-temperature hydrothermal environments (between 60 and 80°C) were members of the *Aquificota* reside.

We hypothesize that the kinetic N isotope effects of ~5–8‰ reported here for *C. mediatlanticus* and *T. ammonificans* will be generally conserved in thermophilic *Campylobacterota* and *Aquificota* using Nap periplasmic NO_3^- reductases during DNRA, regardless of pressure conditions. A slightly higher ε value of ~10‰ has been reported during chemolithoautotrophic denitrification activities, also via a Nap periplasmic NO_3^- reductase, by *S. lithotrophicum* growing as a mesophile at 30°C and 0.2 MPa (Pérez-Rodríguez et al., 2017). These ε values provide a starting point for understanding the contribution of chemolithoautotrophic NO_3^- reduction—either via DNRA or denitrification—to community-level N isotope effects generated in both NO_3^- and NH_4^+ from co-occurring N-based microbial processes at deep-sea hydrothermal vents. Additional understanding of microbial cell concentrations and doubling times associated with chemolithoautotrophic NO_3^- reduction processes in situ, together with considerations relating the substantially lower but consistent supply of NO_3^- from seawater (German & Von Damm, 2003), will be required to establish the extent to which *Campylobacterota* and *Aquificota* define the N biogeochemistry of deep-sea hydrothermal vents.

5 | CONCLUSION

Understanding microbial responses to pressure is complicated by the various techniques used for HHP cultivation, decompression effects, and the diversity of catabolic processes, temperatures, pH, salin and phylogenies investigated along with HHP microbiology. Pressure-based physiologies associated with HHP environments, like deep-sea hydrothermal vents, are further obscured by initial selection and subsequential adaptation processes related to the enrichment and isolation of microorganisms near standard pressure conditions in the laboratory. Results from pure cultures performing chemolithoautotrophic NO_3^- reduction at different pressure conditions show evidence of microbial metabolic adjustments through slower csNRRs and doubling times at higher pressures, while displaying similar NO_3^- processing mechanisms driving N isotope fractionation at all experimental pressures. Robust consistencies in csNRRs, cell yields, and doubling times were also established in relation to temperature conditions between chemolithoautotrophic NO_3^- reducing activities in laboratory pure cultures from deep-sea vent *Campylobacterota* and in deep-sea vent *Campylobacterota* communities growing at HHP conditions. Comparison to previous HHP studies of S^0-oxidizing, Fe(III) reducers and hydrogenotrophic methanogens suggest that higher energy-yielding chemolithoautotrophic reactions experience larger shifts in csRRs and doubling times at increased pressures, as opposed to lower energy-yielding chemolithoautotrophic reactions.

Performing laboratory studies to understand the influence of physicochemical parameters on the physiology and metabolism of anaerobic chemolithoautotrophs also helps to interpret field observations of high-pressure ecosystems, such as deep-sea hydrothermal vents.

ACKNOWLEDGMENTS

This work was supported by Postdoctoral Fellowships from the Geophysical Laboratory, NASA Astrobiology Institute (NAI), the Center for Dark Energy Biosphere Investigations (C-DEBI) Contribution 599 and the University of Pennsylvania Elliman Faculty Fellowship to IPR. Funding was also provided by NSF grants OCE 1038114 (DIF), OCE 1136608 (DIF), BIO-1951673 (DIF), OCE 1038131 (SMS), the WHOI Investment in Science Fund (SMS), and NASA Exobiology Award 80NSSC21K0485 (DIF). We would like to thank Costantino Vetriani (Rutgers University) and Andrew Steele (CIW) for providing the microbial strains and laboratory space, respectively. Special thanks to Roxane Bowden (CIW) for her technical assistance with stable N isotope analyses.

CONFLICT OF INTEREST

The authors declare that they have no conflict of interest.

DATA AVAILABILITY STATEMENT

Microbial strains used are publicly available via international culture collections. All data is available in the supplementary information.

ORCID

Stefan M. Sievert https://orcid.org/0000-0002-9541-2707

REFERENCES

Abe, F. (2007). Exploration of the effects of high hydrostatic pressure on microbial growth, physiology and survival: Perspectives from piezophysiology. *Bioscience, Biotechnology, and Biochemistry*, *71*, 2347–2357.

Balny, C., Mozhaev, V. V., & Lange, R. (1997). Hydrostatic pressure and proteins: Basic concepts and new data. *Comparative Biochemistry and Physiology Part A: Physiology*, *116*, 299–304.

Barlett, D. H., Kato, C., & Horikoshi, K. (1995). High pressure influences on gene and protein expression. *Research in Microbiology*, *146*, 967–706.

Bourbonnais, A., Juniper, S. K., Butterfield, D. A., Devol, A. H., Kuypers, M. M. M., Lavik, G., Hallam, S. J., Wenk, C. B., Chang, B. X., Murdock, S. A., & Lehmann, M. F. (2012). Activity and abundance of denitrifying bacteria in the subsurface biosphere of diffuse hydrothermal vents of the Juan de Fuca ridge. *Biogeosciences*, *9*, 4661–4678.

Bourbonnais, A., Lehmann, M. F., Butterfield, D. A., & Juniper, S. K. (2012). Subseafloor nitrogen transformations in diffuse hydrothermal vent fluids of the Juan de Fuca ridge evidenced by the isotopic composition of nitrate and ammonium. *Geochemistry, Geophysics, Geosystems*, *13*, 1–23.

Breusing, C., Mitchell, J., Delaney, J., Sylva, S. P., Seewald, J. S., Girguis, P. R., & Beinart, R. A. (2020). Physiological dynamics of chemosynthetic symbionts in hydrothermal vent snails. *The ISME Journal*, *14*, 2568–2579.

Campbell, B. J., Engel, A. S., Porter, M. L., & Takai, K. (2006). The versatile *Epsilonproteobacteria*: Key players in sulphidic habitats. *Nature Reviews Microbiology*, *4*, 458–468.

Charlesworth, J., & Burns, B. P. (2016). Extremophilic adaptations and biotechnological applications in diverse environments. *AIMS Microbiology*, *2*, 251–261.

Emerson, D., & Moyer, C. L. (2002). Neutrophilic Fe-oxidizing bacteria are abundant at the Loihi seamount hydrothermal vents and play a major role in Fe oxide deposition. *Applied and Environmental Microbiology*, *68*, 3085–3093.

Fortunato, C. S., Butterfield, D. A., Larson, B., Lawrence-Slavas, N., Algar, C. K., Zeigler Allen, L., Holden, J. F., Proskurowski, G., Reddington, E., Stewart, L. C., Topçuoglu, B. D., Vallino, J. J., & Huber, J. A. (2021). Seafloor incubation experiment with deep-sea hydrothermal vent fluid reveals effect of pressure and lag time on autotrophic microbial communities. *Applied and Environmental Microbiology*, *87*, e00078-21.

Fortunato, C. S., & Huber, J. A. (2016). Coupled RNA-SIP and metatranscriptomics of active chemolithoautotrophic communities at a deep-sea hydrothermal vent. *The ISME Journal*, *10*, 1925–1938.

Foustoukos, D. I., Bizimis, M., Frisby, C., & Shirey, S. B. (2015). Redox controls Ni-Fe-PGE mineralization and re/Os fractionation during serpentinization of abyssal peridotites. *Geochimica et Cosmochimica Acta*, *150*, 11–25.

Foustoukos, D. I., & Pérez-Rodríguez, I. (2015). A continuous culture system for assessing microbial activities in the piezosphere. *Applied and Environmental Microbiology*, *81*, 6850–6856.

Gandhi, H., Wiegner, T. N., Ostrom, P. H., Kaplan, L. A., & Ostrom, N. E. (2004). Isotopic (^{13}C) analysis of dissolved organic carbon in stream water using an elemental analyzer coupled to a stable isotope ratio mass spectrometer. *Rapid Communications in Mass Spectrometry*, *18*, 903–906.

German, C. R., & Von Damm, K. L. (2003). Hydrothermal processes, treatise on. *Geochemistry*, *6*, 181–222.

Giovannelli, D., Sievert, S. M., Hügler, M., Markert, S., Becher, D., Schweder, T., & Vetriani, C. (2017). Insight into the evolution of microbial metabolism from the deep-branching bacterium, *Thermovibrio ammonificans*. *eLife*, *6*, e18990.

Guy, R. D., Fogel, M. L., & Berry, J. A. (1993). Photosynthetic fractionation of the stable isotopes of oxygen and carbon. *Plant Physiology*, *101*, 37–47.

Hoek, J., Canfield, D., Reysenbach, A. L., & Iversen, L. (2006). A bioreactor for growth of sulfate-reducing bacteria: Online estimation of specific growth rate and biomass for the deep-sea hydrothermal vent thermophile *Thermodesulfatator indicus*. *Microbial Ecology*, *51*, 470–478.

Holmes, R. M., McClelland, J. W., Sigman, D. M., Fry, B., & Peterson, B. J. (1998). Measuring ^{15}N–NH_4^+ in marine, estuarine and fresh waters: An adaptation of the ammonia diffusion method for samples with low ammonium concentrations. *Marine Chemistry*, *60*, 235–243.

Houghton, J. L., Seyfried, W. E., Jr., Banta, A. B., & Reysenbach, A. -L. (2007). Continuous enrichment culturing of thermophiles under sulfate and nitrate-reducing conditions and at deep-sea hydrostatic pressures. *Extremophiles*, *11*, 371–382.

Inagaki, F., Takai, K., Nealson, K. H., & Horikoshi, K. (2004). *Sulfurovum lithotrophicum* gen. Nov., sp. nov., a novel sulfur-oxidizing chemolithoautotroph within the *epsilon-Proteobacteria* isolated from Okinawa trough hydrothermal sediments. *International Journal Systematic and Evolutionary Microbiology*, *54*, 1477–1482.

Jannasch, H. W. (1983). Microbial processes at deep sea hydrothermal vents. In P. A. Rona, K. Boström, L. Laubier, & K. L. Smith (Eds.), *Hydrothermal processes at seafloor spreading centers*, *NATO Conference Series (IV Marine Sciences, Volume 12)*. Springer.

Jannasch, H. W. (1995). Microbial interactions with hydrothermal fluids. In S. E. Humphris, R. A. Zierenberg, L. S. Mullineaux, & R. E. Thomson (Eds.), *Seafloor hydrothermal systems: Physical, chemical, biological and geological interactions* (pp. 273–296). American Geophysical Union.

Jebbar, M., Franzetti, B., Girard, E., & Oger, P. (2015). Microbial diversity and adaptation to high hydrostatic pressure in deep-sea hydrothermal vents prokaryotes. *Extremophiles*, *19*, 721–740.

Johnson, C. A., Stricker, C. A., Gulbransen, C. A., & Emmons, M. (2018). Determination of $\delta^{13}C$, $\delta^{15}N$, or $\delta^{34}S$ by isotope-ratio-monitoring mass spectrometry using an elemental analyzer: U. S. *Geological Survey Techniques and Methods*, *D4*, 1–19.

Karl, D. M., Brittain, A. M., & Tilbrook, B. D. (1989). Hydrothermal and microbial processes at Loihi seamount, a mid-plate hot-spot volcano. *Deep Sea Research Part A: Oceanographic Research Papers*, *36*, 1655–1673.

Kendall, C., & Caldwell, E. A. (1998). Fundamentals of isotope geochemistry. In C. Kendall & J. J. McDonnell (Eds.), *Isotope tracers in catchment hydrology* (pp. 51–86). Elsevier Science.

Kinnaman, F. S., Valentine, D. L., & Tyler, S. C. (2007). Carbon and hydrogen isotope fractionation associated with the aerobic microbial oxidation of methane, ethane, propane and butane. *Geochimica et Cosmochimica Acta*, *71*, 271–283.

Kritee, K., Sigman, D. M., Granger, J., Ward, B. B., Jayakumar, A., & Deutsch, C. (2012). Reduced isotope fractionation by denitrification under conditions relevant to the ocean. *Geochimica et Cosmochimica Acta*, *92*, 243–259.

Maggi, F., & Riley, W. (2010). Mathematical treatment of isotopologue and isotopomer speciation and fractionation in biochemical kinetics. *Geochimica et Cosmochimica Acta*, *74*, 1823–1835.

Mariotti, A., Germon, J. C., Hubert, P., Kaiser, P., Letolle, R., Tardieux, A., & Tardieux, P. (1981). Experimental-determination of nitrogen kinetic isotope fractionation - some principles - illustration for the denitrification and nitrification processes. *Plant and Soil*, *62*, 413–430.

Marteinsson, V. T., Moulin, P., Birrien, J., Gambacorta, A., Vernet, M., & Prieur, D. (1997). Physiological responses to stress conditions and barophilic behavior of the hyperthermophilic vent archaeon *Pyrococcus abyssi*. *Applied and Environmental Microbiology*, *63*, 1230–1236.

McNichol, J., Stryhaunyuk, H., Sylva, S. P., Thomas, F., Musat, N., Seewald, J. S., & Sievert, S. M. (2018). Primary productivity below the seafloor at deep-sea hot springs. *Proceedings of the National Academy of Sciences of the United States of America*, *115*, 6756–6761.

McNichol, J., Sylvan, S. P., Thomas, F., Taylor, C. D., Sievert, S. M., & Seewald, J. S. (2016). Assessing microbial processes in deep-sea hydrothermal systems by incubation at in situ temperature and pressure. *Deep Sea Research Part I: Oceanographic Research Papers*, *115*, 221–232.

McQuarrie, D, and Simon, J. D. (1997). Physical chemistry: A molecular approach. University Science Books. *Sausalito*, CA. *P*, 1270.

Meersman, F., Daniel, I., Bartlett, D. H., Winter, R., Hazael, R., & McMillan, P. F. (2013). High-pressure biochemistry and biophysics. *Reviews in Mineralogy and Geochemistry*, *75*, 607–648.

Moyer, C. L., Dobbs, F. C., & Karl, D. M. (1994). Estimation of diversity and community structure through restriction fragment length polymorphism distribution analysis of bacterial 16S rRNA genes from a microbial mat at an active, hydrothermal vent system, Loihi seamount, Hawaii. *Applied and Environmental Microbiology*, *60*, 871–879.

Moyer, C. L., Tiedje, J. M., Dobbs, F. C., & Karl, D. M. (1998). Diversity of deep-sea hydrothermal vent *archaea* from Loihi seamount, Hawaii. *Deep Sea Research Part II: Topical Studies in Oceanography*, *45*, 303–317.

Müller, A. L., Gu, W., Patsalo, V., Deutzmann, J. S., Williamson, J. R., & Spormann, A. M. (2021). An alternative resource allocation strategy in the chemolithoautotrophic archaeon *Methanococcus maripaludis*. *Proceedings of the National Academy of Sciences of the United States of America*, *118*, e2025854118.

Nakagawa, S., & Takai, K. (2008). Deep-sea vent chemoautotrophs: Diversity, biochemistry and ecological significance. *FEMS Microbiology Ecology*, *65*, 1–14.

Nakagawa, S., Takai, K., Inagaki, F., Hirayama, H., Nunoura, T., Horikoshi, K., & Sako, Y. (2005). Distribution, phylogenetic diversity and physiological characteristics of *epsilon-Proteobacteria* in a deep-sea hydrothermal field. *Environmental Microbiology*, *7*, 1619–1632.

Oger, P. M., & Jebbar, M. (2010). The many ways of coping with pressure. *Research in Microbiology*, *161*, 799–809.

Oliver, G. C., Cario, A., & Rogers, K. L. (2020). Rate and extent of growth of a model extremophile, *Archaeoglobus fulgidus*, under high hydrostatic pressures. *Frontiers in Microbiology*, *11*, 1023.

Pérez-Rodríguez, I., Bohnert, K. A., Cuebas, M., Keddis, R., & Vetriani, C. (2013). Detection and phylogenetic analysis of the membrane-bound nitrate reductase (Nar) in pure cultures and microbial communities from deep-sea hydrothermal vents. *FEMS Microbiology Ecology*, *86*, 256–267.

Pérez-Rodríguez, I., Sievert, S. M., Fogel, M. L., & Foustoukos, F. I. (2017). Biogeochemical N signatures from rate-yield trade-offs during in vitro chemosynthetic NO_3^- reduction by deep-sea vent *ε-Proteobacteria* and *Aquificae* growing at different temperatures. *Geochimica et Cosmochimica Acta*, *211*, 214–227.

Schrenk, M. O., Huber, J. A., & Edwards, K. J. (2010). Microbial provinces in the subseafloor. *Annual Review of Marine Science*, *2*, 279–304.

Sedwick, P. N., McMurtry, G. M., & Macdougall, J. D. (1992). Chemistry of hydrothermal solutions from Pele's vents, Loihi seamount, Hawaii. *Geochimica et Cosmochimica Acta*, *56*, 3643–3667.

Seyfried, W. E., Jr., Gordon, P. C., & Dickson, F. W. (1979). A new reaction cell for hydrothermal solution equipment. *American Mineralogist*, *64*, 646–649.

Seyfried, W. E., Jr., Janecky, D. R., & Berndt, M. E. (1987). Rocking autoclaves for hydrothermal experiments II: The flexible cell system. In G. Ulmer & H. Barnes (Eds.), *Experimental hydrothermal techniques* (pp. 216–240). Wiley Interscience.

Sievert, S. M., & Vetriani, C. (2012). Chemoautotrophy at deep-sea vents past, present, and future. *Oceanography*, *25*, 218–233.

Sigman, D. M., Altabet, M. A., Michener, R., McCorkle, D. C., Fry, B., & Holmes, R. M. (1997). Natural abundance-level measurement of the nitrogen isotopic composition of oceanic nitrate: An adaptation of the ammonia diffusion method. *Marine Chemistry*, *57*, 227–242.

Silva, J. L., & Weber, G. (1993). Pressure stability of proteins. *Annual Review of Physical Chemistry*, *44*, 89–113.

Sim, M. S., Ono, S., Donovan, K., Templer, S. P., & Bosak, T. (2011). Effect of electron donors on the fractionation of sulfur isotopes by a marine *Desulfovibrio* sp. *Geochimica et Cosmochimica Acta*, *75*, 4244–4259.

Solorzano, L. (1969). Determination of ammonia in natural waters by phenolhypochlorite method. *Limnology and Oceanography*, *14*, 799–801.

Stetter, K. O., König, H., & Stackebrandt, E. (1983). *Pyrodictium*, a new genus of submarine disc-shaped sulfur reducing archaebacteria growing optimally at 105°C. *Systematic and Applied Microbiology*, *4*, 535–551.

Stewart, L. C., Algar, C. K., Fortunato, C. S., Larson, B. I., Vallino, J. J., Huber, J. A., Butterfield, D. A., & Holden, J. F. (2019). Fluid geochemistry, local hydrology, and metabolic activity define methanogen community size and composition in deep-sea hydrothermal vents. *The ISME Journal*, *13*, 1711–1721.

Sylvan, J. B., Wankel, S. D., LaRowe, D. E., Charoenpong, C. N., Huber, J. A., Moyer, C. L., & Edwards, K. J. (2017). Evidence for microbial mediation of subseafloor nitrogen redox processes at Loihi seamount, Hawaii. *Geochimica et Cosmochimica Acta*, *198*, 131–150.

Takai, K., Miyazaki, M., Hirayama, H., Nakagawa, S., Querellou, J., & Godfroy, A. (2009). Isolation and physiological characterizationof two novel, piezophilic, thermophilic chemolithoautotrophs from a

deep-sea hydrothermal vent chimney. *Environmental Microbiology*, *11*, 1983–1997.

Takai, K., Nakamura, K., Toki, T., Tsunogai, U., Miyazaki, M., Miyazaki, J., Hirayama, H., Nakagawa, S., Nunoura, T., & Horikoshi, K. (2008). Cell proliferation at 122°C and isotopically heavy CH_4 production by a hyperthermophilic methanogen under high-pressure cultivation. *Proceedings of the National Academy of Sciences of the United States of America*, *105*, 10949–10954.

Takai, K., Suzuki, M., Nakagawa, S., Miyazaki, M., Suzuki, Y., Inagaki, F., & Horikoshi, K. (2006). *Sulfurimonas paralvinellae* sp. nov., a novel mesophilic, hydrogen- and sulfur-oxidizing chemolithoautotroph within the *Epsilonproteobacteria* isolated from a deep-sea hydrothermal vent polychaete nest, reclassification of *Thiomicrospira denitrificans* as *Sulfurimonas denitrificans* comb. nov. and emended description of the genus *Sulfurimonas*. *International Journal Systematic and Evolutionary Microbiology*, *56*, 1725–1733.

Taylor, C. D., & Jannasch, H. W. (1976). Subsampling technique for measuring groeth of bacterial cultures under high hydrostatic pressure. *Applied and Environmental Microbiology*, *32*, 355–359.

Topçuoğlu, B. D., Stewart, L. C., Morrison, H. G., Butterfield, D. A., Huber, J. A., & Holden, J. F. (2016). Hydrogen limitation and syntrophic growth among natural assemblages of thermophilic methanogens at deep-sea hydrothermal vents. *Frontiers in Microbiology*, *7*, 1240.

Ver Eecke, H. C., Butterfield, D. A., Huber, J. A., Lilley, M. D., Olson, E. J., Roe, K. K., Evans, L. J., Merkel, A. Y., Cantin, H. V., & Holden, J. F. (2012). Hydrogen-limited growth of hyperthermophilic methanogens at deep-sea hydrothermal vents. *Proceedings of the National Academy of Sciences of the United States of America*, *109*, 13674–13679.

Vetriani, C., Speck, M. D., Ellor, S. V., Lutz, R. A., & Starovoytov, V. (2004). *Thermovibrio ammonificans* sp. nov., a thermophilic, chemolithotrophic, nitrate ammonifying bacterium from deep-sea hydrothermal vents. *International Journal Systematic and Evolutionary Microbiology*, *54*, 175–181.

Vetriani, C., Voordeckers, J. W., Crespo-Medina, M., O'Brien, C. E., Giovanellia, D., & Lutz, R. A. (2014). Deep-sea hydrothermal vent *Epsilonproteobacteria* encode a conserved and widespread nitrate reduction pathway (nap). *The ISME Journal*, *8*, 1510–1521.

Voordeckers, J. W., Starovoytov, V., & Vetriani, C. (2005). *Caminibacter mediatlanticus* sp. nov., a thermophilic, chemolithoautotrophic, nitrate ammonifying bacterium isolated from a deep-sea hydrothermal vent on the mid-Atlantic ridge. *International Journal Systematic and Evolutionary Microbiology*, *55*, 773–779.

Zhang, R., Hedrich, S., Ostertag-Henning, C., & Schippers, A. (2018). Effect of elevated pressure on ferric iron reduction coupled to sulfur oxidation by biomining microorganisms. *Hydrometallurgy*, *178*, 215–223.

Zhang, Y., Li, X., Xiao, X., & Barlett, D. H. (2015). Current developments in marine microbiology: High-pressure biotechnology and the genetic engineering of piezophiles. *Current Opinion in Biotechnology*, *33*, 157–164.

SUPPORTING INFORMATION

Additional supporting information can be found online in the Supporting Information section at the end of this article.

How to cite this article: Pérez-Rodríguez, I., Sievert, S. M., Fogel, M. L., & Foustoukos, D. I. (2022). Physiological and metabolic responses of chemolithoautotrophic NO_3^- reducers to high hydrostatic pressure. *Geobiology*, *00*, 1–13. https://doi.org/10.1111/gbi.12522